Chemosphere 162 (2016) 99–104

Contents lists available at ScienceDirect

Chemosphere

journal homepage: www.elsevier.com/locate/chemosphere

Photoelectrochemical removal of 17β-estradiol using a RuO_2-graphene electrode

Fernando C. Moraes [a, *], Luiz F. Gorup [a], Robson S. Rocha [b], Marcos R.V. Lanza [b], Ernesto C. Pereira [a]

[a] Department of Chemistry, Federal University of São Carlos, P.O. Box 676, C.P. 13560-970 São Carlos, SP, Brazil
[b] Institute of Chemistry of São Carlos, University of São Paulo, P.O. Box 780, C.P. 78060-900 São Carlos, SP, Brazil

HIGHLIGHTS

- A novel material for the electrochemical removal of 17β-estradiol was developed.
- The photoanode based on ruthenium oxide nanoparticles supported on reduced graphene oxide was applied.
- The proposed system was suitable for the removal of 17β-estradiol.

GRAPHICAL ABSTRACT

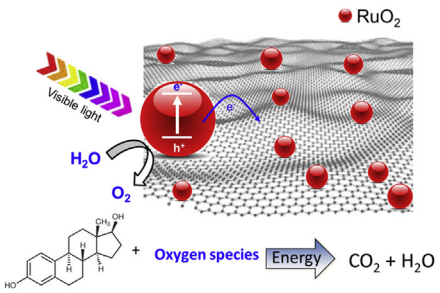

ARTICLE INFO

Article history:
Received 14 June 2016
Received in revised form
19 July 2016
Accepted 23 July 2016
Available online 31 July 2016

Handling Editor: E. Brillas

Keywords:
Photoelectrochemical removal
Reduced graphene oxide
Ruthenium oxide nanoparticles
17β-estradiol

ABSTRACT

A new electrode for the photoelectrochemical removal of 17β-estradiol from water using ruthenium oxide nanoparticles supported on reduced graphene oxide is proposed in this study. The morphology, microstructure and the electrochemical performance of the material were characterized using HRTEM, XRD and Raman spectroscopy. The characterization showed the formation of reduced graphene oxide from a micro-wave assisted hydrothermal method with a particle size of 5.0 nm + 2.4 nm. The electrochemical measurements point to a high performance of the electrode in the presence of a white light source. The hormone removal efficiency in water containing 50 μmol L^{-1} of 17β-estradiol was evaluated using chronoamperometry at +1.0 V and the process was monitored using liquid chromatography. The reaction is pseudo first order with the removal of 92.2% of 17β-estradiol after 60 min of photoelectrocatalytic treatment.

1. Introduction

The occurrence of severe contamination due to an increasing number of compounds indiscriminately discarded via untreated domestic or industrial wastewater discharge became a challenge in the XXI century. In many cases, the damage is relevant, irreversible and can harm human health, as well as animals. One class of such substances that pollute water springs is that of endocrine disruptors (EDs). These substances, even at nanomolar levels, are capable of changing the functioning of the endocrine system, causing different kinds of cancer and damage to the human reproductive system (Hoffman et al., 2003; Sumpter and Johnson, 2005). It has been reported that a specific steroid hormone, the

* Corresponding author.
E-mail address: fcmoraes@hotmail.com (F.C. Moraes).

http://dx.doi.org/10.1016/j.chemosphere.2016.07.070
0045-6535/

17β-estradiol, can cause several problems for animals, of which can be cited: abnormal development of the thyroid, reduction of fertility, sexual disorders and immunological damage in crustaceans, fish, birds and reptiles (Kang et al., 2006). In addition, it has also been reported that the intense exposure of humans to this pollutant lead to several diseases, such as breast and prostate cancer, fertility reduction, congenital formation in children, among others (Ingerslev et al., 2003). All of these environmental impacts generated by 17β-estradiol are due to the bioaccumulation of this disruptor in the aquatic environment, caused by the excretion from animals and humans, followed by the subsequent transport of this chemical by sewage from wastewater treatment stations.

Electrochemical methods based on the remediation of contaminants in wastewaters promote the removal or destruction of pollutant species by redox processes (Steter et al., 2014). This kind of treatment is unique because it offers advantages such as versatility, energy efficiency, ease of automation, costs minimization and chemical stability (Chen and Hung, 2007). Recently, the synthesis of nanostructured materials used in the modification of the surface of electrodes has been the subject of several studies on environmental and electrochemical science. Such modification can increase the sensitivity, selectivity and reproducibility compared to conventional electrodes (Kondalkar et al., 2014). However, the interesting feasible of the nanostructured material applied as water treatment is the photoelectrocatalytic characteristics. These materials have the ability to photogenerate holes on the oxidation of pollutants or even mediate the action to generate hydroxyl radicals. In this sense, several works reported the properties and action of these materials. Dosta and co-workers (Dosta et al., 2016) described the use and photoelectron-catalytic properties of TiO_2 on the development of solar cells. TiO_2 was also employed as material for photoanodes on the photoelectrocatalytic decolorization of acid orange-7-azo dye (Garcia-Segura et al., 2013) and degradation of the drug omeprazole in alkaline media (Tantis et al., 2015). In other system (Cardoso et al., 2016) TiO_2 nanotubes was used as a photoanode coupled with ozonation and achieved 90% of color removal after 15 min of treatment.

Nowadays, one interesting material that can be used in electrochemical sensors is graphene. Graphene nanosheets form a two-dimensional nanostructure with a single layer of sp^2 carbon atoms with a π-conjugated system that leads to special characteristics that can be used in electrochemistry, i.e. high electron mobility (2.0×10^5 cm^2 V^{-1} s^{-1}) allowing fast charge transfer (Du et al., 2008; Baringhaus et al., 2014). Additionally, the graphene acts as a support for the immobilization of several species, especially nanostructured oxides (Seema et al., 2012; Zhou et al., 2012) that can increase its range of application in electrochemical devices (Liu et al., 2012; Cincotto et al., 2014).

It is known that ruthenium oxide (RuO_2) is one of the most prominent species for photo-electrocatalysis, for example, it is used in the oxidation of water to form molecular oxygen (Seema et al., 2012). As RuO_2 can be synthesized as nanostructured particles, it is an interesting compound to be immobilized on the graphene surface (Maeda et al., 2005). Considering the information above, this work aimed to develop and characterize nanostructured materials for building electrodes and measuring their activity in the removal of 17β-estradiol.

2. Experimental

2.1. Chemicals and solutions

All used chemicals were analytical grade.17β-estradiol standard, ruthenium chloride, sodium phosphate and sodium hydrogenphosphate were obtained from Sigma-Aldrich (Germany). 0.1 M phosphate buffer solution (PBS) was used as a supporting electrolyte. All solutions were prepared with water purified in a Millipore Milli-Q system (resistivity > 18.2 MΩ cm). Graphite powder (<20 μm), sodium nitrate, sulfuric acid, nitric acid and potassium permanganate purchased from Sigma-Aldrich (Germany) were used the graphene oxide synthesis. Ethylene-glycol, purchased from Sigma-Aldrich (Germany), and acetone purchased from Synth (Brazil) were used in the hydrothermal micro-wave assisted synthesis. Solvents used in HPLC experiments, such as methanol and ethanol of analytical grade, were obtained from Mallinckrodt (Xalostoc, Edomex, Mexico).

2.2. Apparatus and procedures

Cyclic voltammetry (CV) and linear sweep voltammetry (LSV) experiments were performed using a PGSTAT 302 Autolab electrochemical system (Eco Chemie, Netherlands) monitored with the NOVA software. A conventional electrochemical cell was assembled with three electrodes, in which a glassy carbon electrode (1.0 cm^2 of geometric area) modified with a composite (RGO/RuO_2) was the working electrode, an Ag/AgCl electrode in KCl (3.0 M) was the reference electrode, and a Pt plate was the auxiliary electrode. The electrochemical behavior of 17β-estradiol was evaluated for the proposed electrode by CV and LSV in 0.1 M PBS (pH 7.0) at controlled temperature (25 °C); the scans were collected in a potential range from 0.0 to +0.9 V with a scan rate of 25 mV s^{-1}. The 17β-estradiol removal experiment was performed using chronoamperometry in 0.1 M of PBS (pH 7.0) containing 50.0 μM of 17β-estradiol. The electrolysis experiments were carried out at +1.0 V, in presence and absence of light source from Hg vapor lamp (250 W, high pressure), which implies irradiate system that comprises the range between UV and visible. HPLC experiments were performed in order to determine 17β-estradiol quantitatively. The chromatographic system consisted of a Shimadzu Prominence LC-20AT modular system with two CBM-20A pumps, a CTO-10AS oven, a SIL-20A auto sampler, a SPD-20A variable wavelength detector and an LC-10 Workstation Class data processor (Shimadzu, Japan). The column used was a Phenomenex Luna C-18 (250 mm × 4.6 mm i.d.; 5 μm) protected by a Supelcosil C-18 guard (4.0 mm × 3.0 mm i.d.; 5.0 μm) eluted with mixtures of 65% methanol and 35% water (acidified with formic acid). The chromatographic conditions were 35 °C for the oven temperature, flow rate of 1.0 mL min^{-1}, injection volume of 20.0 μL and UV detection at 280 nm. The morphologies of the RGO and RGO/RuO_2 were examined using high-resolution transmission electron microscopy (HRTEM) micrographs recorded using a Zeiss EM912 Ω STEM (Zeiss, Germany) microscope. The structural characterization was performed by X-ray diffraction (XRD) using a Rigaku Rotaflex Diffractometer model RU200B at 50 kV and 100 mA, with a Cu Kα radiation wavelength in nm of λ = 1.542 A. Raman spectroscopy was carried out using a Horiba/Join Yvon Labran dispersive Raman spectrometer equipped with an Olympus BX41 microscope. The spectra were collected in the range from 1100 to 1850 cm^{-1}, for 10 s and 10 cycles of exposure with excitation at 540 nm using a 10× magnification lens.

2.3. Synthesis of graphene oxide

The Hummers method was used to prepare graphene oxide (GO) (Hummers and Offeman, 1958). For this, graphite powder (10.0 g) was mixed with sodium nitrate (10.0 g) and dispersed in 400.0 mL of concentrated sulphonitric solution (ratio of 1:3 in volume of HNO_3/H_2SO_4). The mixture was kept in an ice bath with magnetic stirring. Then, $KMnO_4$ (50.0 g) was slowly added to the reaction flask and the mixture was left under vigorous stirring for 2 h. After this, the synthesis temperature was controlled at 60 °C, and the

reaction was allowed to continue at this temperature for 30 min. Subsequently, 75.0 mL of H_2O_2 (30% v/v) was added to the system. After the solution became light brown, 1.0 L of HCl solution (10% volume) was added to the mixture, which was kept afterwards in a refrigerator at 4 °C for 24 h. The light brown supernatant was collected and the GO was separated by centrifugation at 10,000 rpm and dried by lyophilization for 24 h.

2.4. Synthesis of RGO/RuO_2 and electrode preparation

The material was prepared using a single mixture of 100.0 mg of GO and 25.0 mg of ruthenium chloride in 80.0 mL of purified water. The mixture was then submitted to microwave-assisted hydrothermal treatment at 160 °C for 15 min. Due to the microwave hot spots, the GO was thermally reduced to RGO and the RuO_2 nanoparticles were obtained. Thus, a suspension containing 5.0 mg RGO/RuO_2 in 1.0 mL of ethanol with 0.5% of Nafion was dropped over a glassy carbon, GC, plate (1.0 cm^2) and dried by lyophilization during 24 h.

3. Results and discussion

3.1. Morphological and structural characterization

The synthesis of the GO and RGO/RuO_2 was evaluated using TEM microscopy. In Fig. 1a, it can be observed that the GO sample shows well-defined nanosheets displayed as a single layer or the overlapping of a few layers. In addition, the GO flakes have a high degree of transparency, indicating that the thickness is small. Regarding the RuO_2 nanoparticles attached to the RGO surface, in Fig. 1b it is clear that the nanoparticles are well-dispersed, with a narrow particle-size distribution that is uniform over the entire graphene surface. Using the Image Photo Pro Plus 6® software, different TEM images of the RGO/RuO_2 were mapped and scanned. The results are presented as a histogram displayed in the inset of Fig. 1b, which shows that the RuO_2 nanoparticles were dispersed as a closed packed monolayer on the RGO nanosheets, with tetragonal shape and a particle size of 5.0 nm + 2.4 nm.

In order to evaluate the crystalline phases of the RuO_2 nanoparticles, XRD patterns were obtained (Fig. 2a). The XRD data of the GO and RGO/RuO_2 presented a typical carbon reflection peak (002) at 15.8°, which can be attributed to the graphitic phase of the graphene oxide. The hexagonal phase (012) of the graphene oxide appeared at 47.8°. The presence of RuO_2 nanoparticles in the composite was characterized by the appearance of diffraction peaks at 39.7°, 65.2°, and 69.4°, which can be readily indexed as (002), (310), and (301), respectively. XRD results were also analyzed using the Scherrer equation (Chen et al., 2012) in order to estimate the mean crystallite sizes of the composite. The estimated mean crystallite size was 5.05 nm for RuO_2, in agreement with TEM data, meaning that each particle is a monocrystal.

The synthesis of GO and the hydrothermal synthesis of RGO/RuO_2 were also evaluated using Raman spectroscopy. Raman scattering has been an efficient method for the identification of single-layer features and edge orientation in graphene. In addition, it is possible to observe the degree of reduction of the samples. It is also possible to perform strain evaluation, determination of doping concentration, and to probe electron-phonon interactions. Also, Raman microscopy can be interesting because some areas of the graphene samples may have different kinds of defects that could show different G-peak frequencies and FWHM, as well as different I_D/I_G ratios (West, 1984).

In Fig. 2b, the Raman spectra collected from the GO sample (black line), RGO (blue line), and RGO/RuO_2 (red line) are presented. The G and D bands at 1605 and 1356 cm^{-1}, respectively, are clearly observed. As expected for the GO sample, the G-band is more intense than the D-band. This behavior is due to the primary mode in sp^2 C-atoms bond, tangential plane stretching (Cong et al., 2010), and the breathing mode of 6 sp^2 carbon rings (Cançado et al., 2011) activated by disorders such as: bond-angle, bond-length, or a heteroatom-induced change in hybridization. Due to crystal symmetry, the D-band is weak in graphene, as expected. However, when D-band magnitudes were evaluated for the RGO and RGO/RuO_2 samples, a large intensity was observed, which is caused by the great number of defects in the material. After the hydrothermal procedure, the GO was reduced to RGO, leading to an inversion of the relative band intensity. The intensity of the D-band increased considerably, while that of the G-band slightly decreased. The I_D/I_G ratio for GO sample was 0.66 and for the RGO/RuO_2 it was 1.32. These values are in agreement with the work reported by Moraes and co-workers (Moraes et al., 2015a,b). that describes a systematic study of the electrochemical reduction of graphene oxide. In GO, sp^3 carbon atoms are bonded to oxygen-containing functional groups, such as hydroxyl, carboxyl, and epoxide. For the GO species, the number of basal-plane graphitic regions is higher than the number of edge-plane regions. As the reduction proceeds (RGO formation) these bonds are broken and oxygenated species are more likely to be removed from the surface; this leads to an increase in the I_D/I_G ratio. The same behavior was observed when RuO_2 nanoparticles were incorporated over RGO. The hydrothermal reduction process generates an increase in the number of edge plane defects in the graphene layers (Sato et al., 2006; Kaniyoor and Ramaprabhu, 2012). These lattice defects and the presence of the oxide nanoparticles have a direct influence in the electron mobility of the sample, improving this composite to be used as electrodic material.

3.2. Electrochemical behavior of 17β-estradiol

The study of the electrochemical behavior of 17β-estradiol at the

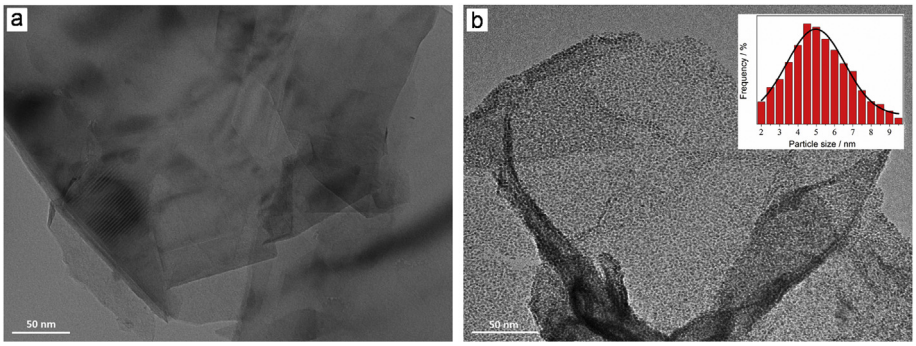

Fig. 1. (a) TEM image of GO nanosheets. (b) TEM image of the composite RGO/RuO_2. Inset: histogram of RuO_2 particle size.

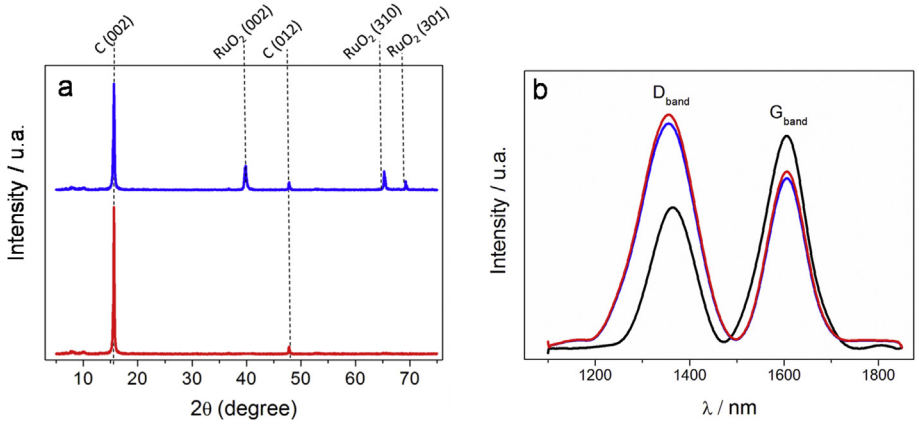

Fig. 2. (a) XRD patterns for GO (red line) and RGO/RuO_2 (blue line). (b) Raman spectra of GO (black line), RGO (blue line) and RGO/RuO_2 (red line). (For interpretation of the references to color in this figure legend, the reader is referred to the web version of this article.)

RGO/RuO_2 electrode was performed using cyclic voltammetry in presence and absence of 17β-estradiol, with a scan rate of 25 mV s^{-1}, as displayed in Fig. 3. In the potential range studied, only one oxidation process was observed. This oxidation peak could be attributed to an irreversible oxidation of the hydroxyl group present in the aromatic ring of the 17β-estradiol molecule to form a ketone species (Ngundi et al., 2003); this is illustrated by the mechanism presented in the inset in Fig. 3.

In order to evaluate the effects of the photovoltaic properties of the RGO/RuO_2 system, the electro-oxidation of 17β-estradiol was carried out using LSV in the dark and in the presence of light (Fig. 4). The voltammograms were collected using the RGO/RuO_2 electrode in 0.1 M PBS (pH 7.0) containing 50.0 μM of 17β-estradiol in the absence and in the presence of a source of light, as described in the Experimental section. The electrochemical measurements were carried out in a potential range that varied from +0.4 to +1.1 V with a scan rate of 25 mV s^{-1}.

It is evident in Fig. 4 that the current peak, attributed to 17β-estradiol oxidation, increased 3.5-fold in the presence of light compared with the same measurement in the dark. This increase in the current of the hormone oxidation process could be attributed to a mechanism based on semiconductor-mediated photo-degradation initiated by the surface electron injection (denoted as SMPD) (Chen et al., 2010). In this sense, it was recognized that the RuO_2 acts as a good oxidation catalyst for oxygen evolution because of the particularly low overvoltage (closed to +0.4 V) (Miles et al., 1978) and because RuO_2 has often been used in photocatalytic water-splitting systems, especially in light-induced systems (Banerjee and Mukherjee, 2014). In this case, the hybrid material (RGO/RuO_2), in the presence of visible light, absorbed more energy than the band gap of the semiconductor, exciting electrons from the valence band to the conduction band. The band-band excitation produces reductive conduction band electrons (e^-_{cb}) and oxidative band holes (h^+_{vb}). The holes can react with surface-adsorbed H_2O, producing hydroxyl radicals (•OH – equation (1)). In aerated systems, the e^-_{cb} electrons are usually scavenged by O_2 to yield superoxide radical anions ($\bullet O_2^-$ - equation (2)) (Chen et al., 2010). This way, both O_2 and the oxygenated radicals are activated on the surface of the hybrid material. In the proposed RGO/RuO_2 photoanode, the holes are photochemically generated at the RuO_2 surface that react with water to generate hydroxyl radicals that later react with 17b-estradiol

$$H_2O + h_{vb}{}^+ \rightarrow \cdot OH + H^+ \quad (1)$$

$$O_2 + e_{cb}{}^- \rightarrow \cdot O_2{}^- \quad (2)$$

With the electrode polarized at +1.0 V, 17β-estradiol could be

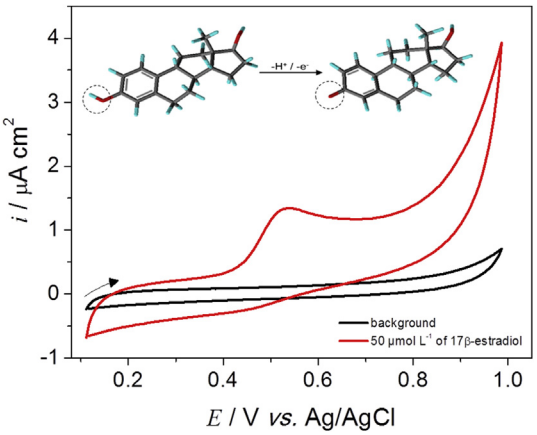

Fig. 3. Cyclic voltammograms for the RGO/RuO_2 film electrode in absence (black line) and presence of 50.0 μM of 17β-estradiol (red line), using a scan rate at 25 mV s^{-1}. Inset: Mechanism of 17β-estradiol oxidation. (For interpretation of the references to color in this figure legend, the reader is referred to the web version of this article.)

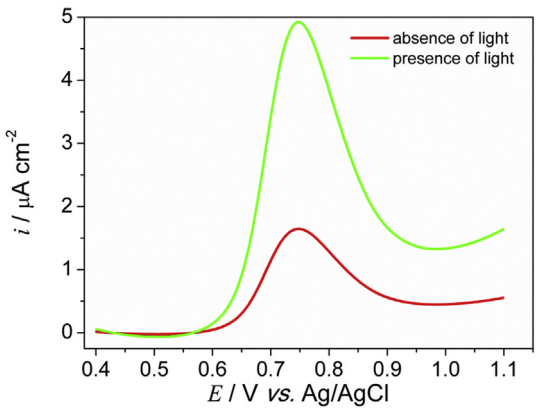

Fig. 4. LSV response of RGO/RuO_2 in n 0.1 M PBS (pH 7.0) containing 50.0 μM of 17β-estradiol under different conditions: in the dark (red line) and in the presence of a source of visible light (green line), with a scan rate at 25 mV s^{-1}. (For interpretation of the references to color in this figure legend, the reader is referred to the web version of this article.)

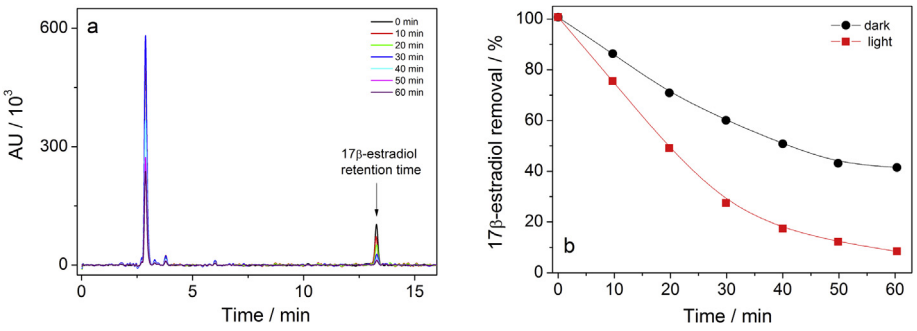

Fig. 5. (a) Chromatograms sample in presence of 50.0 μM of 17β-estradiol, using the RGO/RuO_2 electrode in presence of light. (b) Kinetics of degradation of 17β-estradiol in 60 min using the electrode RGO/RuO_2 in light and dark.

oxidized in two paths, which may occur currently. First is the direct electro-oxidation hydroxyl group present in the aromatic ring of the 17β-estradiol molecule (Ngundi et al., 2003; Moraes et al., 2015a,b). Also, it was reported that the 17β-estradiol electro-oxidation could form a polymeric product (Murugananthan et al., 2007; Yoshihara and Murugananthan, 2009). However, the hydroxyl radicals generated on the RGO/RuO_2 surface may oxidize the polymeric product leading to an efficient degradation of the hormone, as described by Brocenschi and co-workers (Brocenschi et al., 2016). In this sense, this proposed chemical mechanism and the electrochemical steps allow for a large increase in the current of the oxidation peak that can lead to an effective system of 17β-estradiol degradation.

3.3. 17β-estradiol electrochemical removal

The 17β-estradiol removal experiment was performed using chronoamperometry in 0.1 M of PBS (pH 7.0) containing 50.0 μM of 17β-estradiol. The electrolysis experiments were monitored using HPLC with the conditions described in the Experimental section. The RGO/RuO_2 electrode was polarized at +1.0 V, and aliquots of 500 μL of the sample were directly collected from the electrochemical cell using a peristaltic pump and were injected in the chromatograph. The sampling was carried out every 10 min. In Fig. 5a, the chromatograms of the samples revealed a 17β-estradiol peak recorded in 13.3 min. After the electrolysis, a sharp decrease in the 17β-estradiol peak was observed indicating a strong removal of the 17β-estradiol from the sample using the electrode prepared with RGO/RuO_2 in presence of light. To compare the efficiency of the proposed photo-electrochemical system of 17β-estradiol removal, the electrolysis of the hormone was carried out in the presence and absence of light. Considering the area of the peak related to 17β-estradiol, kinetic curves were plotted based on the percentage of removal as a function of the electrolysis time, as displayed in Fig. 5b. It was observed that the RGO/RuO_2 electrode, in the absence of light and after 60 min, achieved a percentage of hormone degradation of 59.5%. However, the presence of light promoted a removal of 92.2% of the 17β-estradiol after 60 min of photoelectrocatalytic treatment under pseudo first order kinetics. Therefore, the use of RGO/RuO_2 as a material for the development of photoelectrochemical methods could be a promising alternative for the remediation of the endocrine disruptor in the environment.

4. Conclusions

A semiconductor material for the development of a photo-electrochemical device to remove 17β-estradiol was proposed in this work. The hydrothermal method with micro-wave assistance was efficient for the preparation of the RGO/RuO_2 material. The proposed material was successfully characterized by HRTEM, XRD, and Raman microscopy, which indicated that GO was hydrothermally reduced and that RuO_2 nanoparticles of small size were supported with uniform distribution. The voltammetric experiments in the presence of light demonstrated that the 17β-estradiol oxidation process has a mechanism based on semiconductor-mediated photo-degradation initiated by surface electron injection. Therefore, the electronic properties of the proposed hybrid material show great efficiency in the electro-oxidation of the endocrine disruptor yielding excellent values for the percentage of 17β-estradiol removal.

Acknowledgments

The financial support of CAPES, FAPESP (2013/07296-2) and CNPq is acknowledged.

References

Banerjee, T., Mukherjee, A., 2014. Overall water splitting under visible light irradiation using nanoparticulate RuO_2 loaded Cu_2O powder as photocatalyst. Energy Proced. 54, 221–227.
Baringhaus, J., Ruan, M., Edler, F., Tejeda, A., Sicot, M., Taleb-Ibrahimi, A., Li, A.P., Jiang, Z., Conrad, E.H., Berger, C., Tegenkamp, C., De Heer, W.A., 2014. Exceptional ballistic transport in epitaxial graphene nanoribbons. Nature 4, 349–354.
Brocenschi, R.F., Rocha-Filho, R.C., Bocchi, N., Biaggio, S.R., 2016. Electrochemical degradation of estrone using a boron-doped diamond anode in a filter-press reactor. Electrochim. Acta 197, 186–193.
Cançado, L.G., Jorio, A., Ferreira, E.H.M., Stavale, F., Achete, C.A., Capaz, R.B., Moutinho, M.V.O., Lombardo, A., Kumala, T.S., Ferrari, A.C., 2011. Quantifying defects in graphene via Raman spectroscopy at different excitation energies. Nano Lett. 11, 3190–3196.
Cardoso, J.C., Bessegato, G.G., Zanoni, M.V.B., 2016. Efficiency comparison of ozonation, photolysis, photocatalysis and photoelectrocatalysis methods in real wastewater decolorization. Water Res. 98, 39–46.
Chen, G., Hung, Y.T., 2007. Electrochemical wastewater treatment processes. Adv. Physicochem. Treat. Technol. 5, 57–106.
Chen, C., Ma, W., Zhao, J., 2010. Semiconductor-mediated photodegradation of pollutants under visible-light irradiation. Chem. Soc. Rev. 39, 4206–4219.
Chen, Y., Zhang, X., Zhang, D., Ma, Y., 2012. One-pot hydrothermal synthesis of ruthenium oxide nanodots on reduced graphene oxide sheets for supercapacitors. J. Alloy Compd. 511, 251–256.
Cincotto, F.H., Moraes, F.C., Machado, S.A.S., 2014. Graphene nanosheets and quantum dots: a smart material for electrochemical applications. Chem. Eur. J. 20, 4746–4753.
Cong, C., Yu, T., Wang, H., 2010. Raman study on the G mode of graphene for determination of edge orientation. ACS Nano 4, 3175–3180.
Dosta, S., Robotti, M., Garcia-Segura, S., Brillas, E., Cano, I.G., Guilemany, J.M., 2016. Influence of atmospheric plasma spraying on the solar photoelectro-catalytic properties of TiO_2 coatings. Appl. Catal. B-Environ 189, 151–159.
Du, X., Skachko, I., Baker, A., Andrei, E., 2008. Approaching ballistic transport in suspended graphene. Nat. Nanotech. 3, 491–495.
Garcia-Segura, S., Dosta, S., Guilemany, J.M., Brillas, E., 2013. Solar photoelectrocatalytic degradation of Acid Orange 7 azo dye using a highly stable TiO_2 photoanode synthesized by atmospheric plasma spray. Appl. Catal. B-Environ 132, 142–150.
Hoffman, D.J., Rattner, B.A., Burton Jr., G.A., Cairns Jr., J., 2003. Handbook of Ecotoxicology. Lewis Publishers CRC Press, USA, pp. 1033–1098.

Hummers, W.S., Offeman, R.E., 1958. Preparation of graphitic oxide. J. Am. Chem. Soc. 80, 1339.
Ingerslev, F., Vaclavik, E., Halling-Sorensen, B., 2003. Pharmaceuticals and personal care products - a source of endocrine disruption in the environment. Pure Appl. Chem. 75, 1881–1893.
Kang, J.H., Kondo, F., Katayama, Y., 2006. Human exposure to bisphenol A. Toxicology 226, 79–89.
Kaniyoor, A., Ramaprabhu, S., 2012. A Raman spectroscopic investigation of graphite oxide derived graphene. AIP Adv. 2, 1–13.
Kondalkar, V.V., Mali, S.S., Mane, R.M., Dandge, P.B., Choudhury, S., Hong, C.K., Patil, P.S., Patil, S.R., Kim, J.H., Bhosale, P.N., 2014. Photoelectrocatalysis of cefotaxime using nanostructured TiO_2 photoanode: identification of the degradation products and determination of the toxicity level. Ind. Eng. Chem. Res. 53, 18152–18162.
Liu, S., Tian, J., Wang, L., Luo, Y., Sun, X., 2012. One-pot synthesis of CuO nanoflower-decorated reduced graphene oxide and its application to photocatalytic degradation of dyes. Catal. Sci. Tech. 2, 339–344.
Maeda, K., Takata, T., Hara, M., Saito, N., Inoue, Y., Kobayashi, H., Domen, K., 2005. GaN: ZnO solid solution as a photocatalyst for visible-light-driven overall water splitting. J. Am. Chem. Soc. 127, 8286–8287.
Miles, M.H., Klaus, E.A., Gum, B.P., Laker, J.R., Serafin, W.E., Srinivasan, S., 1978. The oxygen evolution reaction on platinum, iridium, ruthenium and their alloys at 80 °C in acid solutions. Electrochim. Acta 23, 521–526.
Moraes, F.C., Freitas, R.G., Pereira, R., Gorup, L.F., Cuesta, A., Pereira, E.C., 2015a. Coupled electronic and morphologic changes in graphene oxide upon electrochemical reduction. Carbon 91, 11–19.
Moraes, F.C., Rossi, B., Donatoni, M.C., de Oliveira, K.T., Pereira, E.C., 2015b. Sensitive determination of 17β-estradiol in river water using a graphene based electrochemical sensor. Anal. Chim. Acta 881, 37–43.
Murugananthan, M., Yoshihara, S., Rakuma, T., Uehara, N., Shirakashi, T., 2007. Electrochemical degradation of 17β-estradiol (E2) at boron-doped diamond (Si/BDD) thin film electrode. Electrochim. Acta 52, 3242–3249.
Ngundi, M.M., Sadik, O.A., Yamaguchi, T., Suye, S., 2003. First comparative reaction mechanisms of β-estradiol and selected environmental hormones in a redox environment. Electrochem. Commun. 5, 61–67.
Sato, K., Saito, R., Oyama, Y., Jiang, J., Cançado, L.G., Pimenta, M.A., Jorio, A., Samsonidze, G.G., Dresselhaus, G., Dresselhaus, M.S., 2006. D-band Raman intensity of graphitic materials as a function of laser energy and crystallite size. Chem. Phys. Lett. 427, 117–121.
Seema, H., Kemp, K.C., Chandra, V., Kim, K.S., 2012. Graphene-SnO_2 composites for highly efficient photocatalytic degradation of methylene blue under sun light. Nanotechnology 23, 355705.
Steter, J.R., Barros, W.R.P., Lanza, M.R.V., Motheo, A.J., 2014. Electrochemical and sonoelectrochemical processes applied to amaranth dye degradation. Chemosphere 117, 200–207.
Sumpter, J.P., Johnson, A.C.L., 2005. Lessons from endocrine disruption and their application to other issues concerning trace organics in the aquatic environment. Environ. Sci. Technol. 39, 4321–4332.
Tantis, I., Bousiako, L., Frontistis, Z., Mantzavinos, D., Konstantinou, I., Antonopoulou, M., Karikas, G.A., Lianos, P., 2015. Photocatalytic and photoelectrocatalytic degradation of the drug omeprazole on nanocrystalline titania films in alkaline media: effect of applied electrical bias on degradation and transformation products. J. Hazard. Mater 294, 57–63.
West, A.R., 1984. Solid State Chemistry and its Applications. Wiley, New York.
Yoshihara, S., Murugananthan, M., 2009. Decomposition of various endocrine-disrupting chemicals at boron-doped diamond electrode. Electrochim. Acta 54, 2031–2038.
Zhou, X., Shi, T., Zhou, H., 2012. Hydrothermal preparation of ZnO-reduced graphene oxide hybrid with high performance in photocatalytic degradation. Appl. Surf. Sci. 258, 6204–6211.